Received: 24 July 2020 | Accepted: 27 October 2020

DOI: 10.1111/gcb.15436

PRIMARY RESEARCH ARTICLE

Global Change Biology WILEY

Divergent expression of hypoxia response systems under deoxygenation in reef-forming corals aligns with bleaching susceptibility

Rachel Alderdice[1] | David J. Suggett[1] | Anny Cárdenas[2] | David J. Hughes[1] | Michael Kühl[1,3] | Mathieu Pernice[1] | Christian R. Voolstra[2]

[1]Climate Change Cluster, Faculty of Science, University of Technology Sydney, Ultimo, NSW, Australia

[2]Department of Biology, University of Konstanz, Konstanz, Germany

[3]Marine Biology Section, Department of Biology, University of Copenhagen, Helsingør, Denmark

Correspondence
Rachel Alderdice, Climate Change Cluster, Faculty of Science, University of Technology Sydney, Ultimo, NSW 2007, Australia.
Email: Rachel.Alderdice@student.uts.edu.au

Christian R. Voolstra, Department of Biology, University of Konstanz, 78457 Konstanz, Germany.
Email: christian.voolstra@uni-konstanz.de

Funding information
Australian Research Council, Grant/Award Number: DP180100074; Gordon and Betty Moore Foundation, Grant/Award Number: GBMF9206; Deutsche Forschungsgemeinschaft, Grant/Award Number: 433042944

Abstract

Exposure of marine life to low oxygen is accelerating worldwide via climate change and localized pollution. Mass coral bleaching and mortality have recently occurred where reefs have experienced chronic low oxygen events. However, the mechanistic basis of tolerance to oxygen levels inadequate to sustain normal functioning (i.e. hypoxia) and whether it contributes to bleaching susceptibility, remain unknown. We therefore experimentally exposed colonies of the environmentally resilient *Acropora tenuis*, a common reef-building coral from the Great Barrier Reef, to deoxygenation–re-oxygenation stress that was aligned to their natural night–day light cycle. Specifically, the treatment involved removing the 'night-time O_2 buffer' to challenge the inherent hypoxia thresholds. RNA-Seq analysis revealed that coral possess a complete and active hypoxia-inducible factor (HIF)-mediated hypoxia response system (HRS) homologous to other metazoans. As expected, *A. tenuis* exhibited bleaching resistance and showed a strong inducibility of HIF target genes in response to deoxygenation stress. We applied this same approach in parallel to a colony of *Acropora selago*, known to be environmnetally susceptible, which conversely exhibited a bleaching phenotype response. This phenotypic divergence of *A. selago* was accompanied by contrasting gene expression profiles indicative of varied effectiveness of their HIF-HRS. Based on our RNA-Seq analysis, we propose (a) that the HIF-HRS is central for corals to manage deoxygenation stress and (b) that key genes of this system (and the wider gene network) may contribute to variation in coral bleaching susceptibility. Our analysis suggests that heat shock protein (hsp) 70 and 90 are important for low oxygen stress tolerance and further highlights how hsp90 expression might also affect the inducibility of coral HIF-HRS in overcoming a metabolic crisis under deoxygenation stress. We propose that differences in coral HIF-HRS could be central in regulating sensitivity to other climate change stressors—notably thermal stress—that commonly drive bleaching.

KEYWORDS

bleaching, coral reef, hypoxia stress, metabolic crisis, ocean deoxygenation, stress regulation

1 | INTRODUCTION

Ocean warming and coastal eutrophication are driving the dissolved oxygen (O_2) inventory below levels required to meet biological O_2 demands of many cornerstone marine life forms (Hughes et al., 2020; Jackson, 2008; Keeling et al., 2010). Ocean deoxygenation of up to 7% globally, relative to current levels, is predicted by 2100 under different climate change scenarios (Keeling et al., 2010). Such declines in dissolved O_2 will, in turn, amplify the frequency and intensity with which marine life is subjected to O_2 supply insufficient for normal biological functioning (i.e. hypoxia; Breitburg et al., 2018; Schmidtko et al., 2017).

Reef-building corals in shallow tropical reefs already persist under highly dynamic O_2, pH, temperature, and nutrient regimes (Greenstein & Pandolfi, 2008; Hoegh-Guldberg et al., 2007), suggesting an inherently evolved capacity to thrive under routine low O_2 cellular supply (Camp et al., 2017). Complex metabolic interplay among the cnidarian host and the microbial symbionts living within its tissues (Matthews et al., 2018; Xiang et al., 2020) and skeleton (Bernasconi et al., 2019; Pernice et al., 2020; Ricci et al., 2019) further drive O_2 fluctuations in coral tissue from hyperoxia during the day to hypoxia throughout the night (Kühl et al., 1995, 2008). However, recent natural deoxygenation events on reefs have resulted in high coral bleaching-induced mortality via transient hypoxia (Altieri et al., 2017), a phenomenon akin to the globally recognized mass coral bleaching events under transient heat waves (Hughes et al., 2018). The extent with which corals are at risk from future declines in background O_2 saturation will rest on the extent and scope of their hypoxia detection and hypoxia response systems (HRS)—a process that remains at present entirely unknown (Hughes et al., 2020).

Cellular detection of reduced O_2 levels from ion channel modulation is highly conserved in both plants and animals (López-Barneo et al., 2001; Wang et al., 2017). However, the molecular repertoire orchestrating HRS varies across kingdoms, whereby ethylene response factor (ERF-VII) and hypoxia-inducible factor (HIF) act as the master transcriptional regulators, respectively (Hammarlund et al., 2020; Schmidt et al., 2018). In metazoans, the hypoxia-inducible factor subunit alpha (HIFα) and prolyl hydrolyse domains (PHDs) form the primary functional axis of the HRS (Kaelin & Ratcliffe, 2008; Loenarz et al., 2011; Rytkönen et al., 2011). HIFα is constitutively transcribed via a series of signalling events by growth factors and kinases (receptor tyrosine kinase [RTK], phosphatidylinositol-4, 5-bisphosphate-3-kinase [PI3K], mitogen-activated protein kinases [MAPK] and mammalian target of rapamycin [mTOR]; Bruick & McKnight, 2001; Glück et al., 2015).

The fate of HIFα is primarily regulated by the cellular O_2 microenvironment. HIFα degradation involves PHD proteins under normoxia, but as O_2 availability becomes increasingly limited, PHD degradation capacity is disrupted and HIFα can accumulate (Kaelin & Ratcliffe, 2008). HIFα proteins reach their governing potential once in the nucleus, forming part of the 'active HIF complex' together with HIFβ subunit, cAMP response element binding protein (CREB/p300) and hypoxia-responsive elements (HREs). Heat shock protein 90 (hsp90) also directly interacts with HIFα, acting as a protein stabilizer and induces conformational changes in its structure critical for coupling with HIFβ to form the 'active HIF complex' (Gradin et al., 1996; Hur et al., 2002; Isaacs et al., 2002; Katschinski et al., 2004). Cohorts of genes are then targeted for transcription by the 'active HIF complex' to activate hypoxia stress-mitigating mechanisms (Dengler et al., 2014), mainly directed at remodelling mitochondrial activity. Metabolic reprogramming is enabled by HIF-regulated glycolytic enzymes (pyruvate dehydrogenase kinase [PDK] and lactate dehydrogenase A [LDHA], enolase [ENO1], glyceraldehyde phosphate dehydrogenase [GAPDH], fructose-bisphosphate aldolase [ALDO], hexokinase [HK] and phosphofructokinase [PFK] to promote anaerobic respiration while demoting tricarboxylic acid cycle (TCA) activity in the mitochondria (Benita et al., 2009). HIF also selectively targets PTEN-induced kinase-1/Parkin-mediated mitophagy via balances of the anti-death protein B-cell lymphoma 2 (Bcl2) and the pro-death protein Bcl2 nineteen-kilodalton interacting protein (BNIP3; Yang et al., 2009; Zhang & Ney, 2009). Both mechanisms provide a means to reduce levels of detrimental mitochondrial reactive oxygen species (ROS) and to encourage remodelling of bioenergetic pathways in the absence of O_2 in an attempt to sustain metabolic demands (Thomas & Ashcroft, 2019). Such a means of hypoxia management appears essential for corals attempting to alleviate bleaching under environmental stress; for example, host mitophagy (Dunn et al., 2012) and an upregulation of glycolytic enzymes (Leggat et al., 2011) as a response to thermal stress. Similarly, cellular hypoxia management is generally accompanied by systems dissipating ROS (Blokhina et al., 2003; Lushchak & Bagnyukova, 2006). Most metazoans have procured a network of antioxidant enzymes to coordinate redox homeostasis by detoxifying ROS by-products of mitochondrial respiration, and efficient control of ROS accumulation is considered essential in mitigating physiological cascades that result in coral bleaching under thermal stress (Suggett & Smith, 2020). Furthermore, light-independent coral bleaching (DeSalvo et al., 2012; Tolleter et al., 2013), when cells are in a hypoxic state, would suggest that regulation of an HIFα-mitochondrial system in corals is thus integral to their capacity to respond to stress by reducing mitochondrial ROS production rather than promoting ROS detoxification. Consequently, identifying the genes acting as 'effectors' in coral HRSs could also help unravel the inherent molecular regulation of coral susceptibility to cascades of warming, acidification and hypoxia events (Hughes et al., 2020).

Evolutionary divergence of 'hypoxia effector genes', for example, HIF has likely been influenced by the extent of cellular compartmentalization, which ultimately plays a role in O_2 availability (Gabaldón & Pittis, 2015). While HIF indeed appears present in reef-building corals based on transcriptome mining (DeSalvo et al., 2012; Levy et al., 2011; Ruiz-Jones & Palumbi, 2015; Yum et al., 2017; Zoccola et al., 2017), it may not necessarily be functionally active to hypoxia, as evident for marine invertebrates such as *Tigriopus californicus* subjected to highly variable O_2 availability (Graham & Barreto, 2019). Consequently, it is unclear whether corals drive their HRS via a

functional HIF similar to other metazoans or rather conform to the 'earliest metazoans' (i.e. Porifera) that simply rely on O_2-dependent enzymes and sulphides (Mills et al., 2018; Rytkönen et al., 2011).

To identify the gene suite responsible for the HRS of the reef-forming coral *Acropora tenuis* (common to the Great Barrier Reef, GBR), we conducted a deoxygenation–reoxygenation stress experiment aligned to their natural night–day light cycle, with time-series sampling for bleaching indicators (cell density and Chlorophyll *a* and c_2 content) and RNA-Seq analysis. Specifically, we subjected replicate genets to deoxygenated seawater at night-time—that is, coinciding with their routine cycle of intra-tissue deoxygenation (Kühl et al., 1995). Removal of their 'night-time O_2 buffer' (NTOB) was intended to challenge inherent hypoxia thresholds and intensify their oxygen debt state. The coral species, *A. tenuis*, was reported in the 2016–2017 mass bleaching events on the GBR (Hughes et al., 2017) to exhibit inherently greater capacity to resist heat stress-induced bleaching compared to the closely related *Acropora selago* (Hoogenboom et al., 2017). Thus, following the same experimental design in parallel using clonal ramets from a bleaching-susceptible *A. selago* colony, we explored whether any deviations to the HIF-driven stress regulation occurred compared to the more stress-resistant species, *A. tenuis*.

2 | MATERIALS AND METHODS

2.1 | Experimental design

Coral fragments (~4 cm in length) were collected from *A. tenuis* and *A. selago* colonies in November 2018 originating from the northern GBR (Vlasoff Reef). A replicate coral fragment of *A. tenuis* was taken from each of five separate neighbouring colonies ($n = 5$ genets), whereas five replicate fragments for *A. selago* were taken from fragmentation of a single colony ($n = 5$ ramets) due to limited colony availability. As such, our experiment was conducted within the constraints of the different replication, with the aim to build knowledge of the HIF-HRS from *A. tenuis* colonies but subsequently explored in the context of a different species colony with known differences in heat-induced bleaching susceptibility. Examining intracolonial genetic variability in corals has indeed been shown previously to provide validation for genetic analyses on replicates from a single coral colony for evidence of divergent stress responses (Schweinsberg et al., 2015).

All coral replicates were acclimated for >1 week in a shaded main system outdoor closed-circulation aquarium (James Cook University, Cairns; 22–40°C min–max daily air temperature range, average water temperature of 28°C and dissolved oxygen [DO] of ~6 mg O_2/L maintained via continuous aeration) before moving fragments to experimental incubation chambers in late November 2018. Incubation conditions were then established to mimic in situ reef conditions from where corals were sourced, with the exception of DO concentration. Deoxygenated treatment was achieved via flushing of seawater with N_2 prior to additional flushing with CO_2 to account for subsequent increase in pH as per Klein et al. (2017). Both control and treatment conditions consisted of diel time of day alignment, maintenance in closed vessels to drive continuous O_2 drawdown throughout the night and subsequent reoxygenation in open vessels under daylight (returning to their starting DO level of ~6 mg O_2/L). Deoxygenation stress treatment was superimposed onto the ambient night-time intra-tissue hypoxia (Kühl et al., 1995), and so removal of the inherent 'NTOB' to drive intensification of an O_2 debt state. It is currently unknown the duration of either acute or chronic hypoxia events on reefs (Hughes et al., 2020), and we therefore employed a relatively short exposure time (12-hr deoxygenation) compared to those typically used for heat stress studies (1–2 weeks; Bellantuono et al., 2012) given that our experiment was designed to initiate and capture the gene response to low O_2 stress without the coral potentially acclimating to the stress (e.g. in the case of the more tolerant species), and that the sensitivity in gene regulation in response to the loss of O_2 is likely to be greater for an organism compared to heat stress (López-Barneo et al., 2001).

Incubation set up consisted of 10 × 4 L transparent screw-top vessels (five for each of control and treatment) placed in a large water bath, with each coral species sampled on consecutive days. Pumps were installed in the vessels to ensure sufficient mixing and to minimize diffusive boundary layer thickness. To prevent build-up of waste products in the seawater over time, we utilized a large water volume to biomass ratio (Camp et al., 2015), with three coral fragments per 5 × 4 L control and 5 × 4 L treatment incubation vessels. Temperature was maintained at 28°C using 2 × 300 W aquarium bar heaters. A photon scalar irradiance (PAR, 400–700 nm) of ~180 μmol photons m^{-2} s^{-1} (with 4 hr ramp) was provided by Hydra52 LEDs and measured with a calibrated underwater scalar irradiance sensor (LiCor LI-193) connected to a light meter (LiCor Li-250A). Dark conditions were created by black-out material placed over the incubation vessels throughout the 12 hr night period and vessel lids were sealed with parafilm. In this way, we allowed for a continued lowering of both DO and pH, as recommended by Klein et al. (2017) to study hypoxia during night-time with appropriate ecological relevance (see corresponding time point pH data in Figure S1). This was followed by a 12 hr 'recovery' phase in the light with opened vessels to promote reoxygenation via water surface agitation with the ambient air. Samples were collected from acclimation tanks for T0 ~ 1 hr prior to deoxygenation exposure, 0.5 hr into (T1) and at the end (12 hr, T2) of the deoxygenation night-time phase, and finally after 12 hr exposure in the light (T3). This 12 hr 'recovery' phase, where both control and treatment experienced LED light exposure and 'normal' DO levels were critical to determine the recovery capacity after exposure to the different low O_2 exposures. One coral fragment from each vessel was removed at each time point T1–T3 (as well as from the acclimation system at T0) and immediately snap-frozen for subsequent molecular analysis. Further details of experimental design and corresponding measured O_2 and pH for each incubation chamber across time points are provided in Figure S2 and Table S1a–c.

2.2 | Chlorophyll extraction and cell density

Coral tissue was air-picked from the skeleton using a sterile filtered airflow from a 1 ml pipette tip connected via a rubber hose to a bench top air pressure valve and approximately 10 ml of PBS. For each coral sample, Symbiodiniaceae cell density was counted three times using a Neubauer counting chamber as per Camp et al. (2019; Table S2a,b). A 10 ml subsample was taken from each homogenate, immediately centrifuged at 6000 *g* for 10 min (4°C) and the supernatant removed. The pellet containing the Symbiodiniaceae was sonicated then resuspended in 100% acetone for 24 hr (at 4°C) in the dark to extract chlorophylls *a* and c_2. The extracts were centrifuged at 10,000 *g* for 15 min and absorbance was read at 630, 663 and 750 nm. Chlorophyll concentrations were determined according to the spectrometric equations for dinoflagellates (Jeffrey & Humphrey, 1975; Data S3). Chlorophylls *a* and c_2 are given as total chlorophyll (Table S3a,b). All measurements were normalized to skeletal surface area, determined via the paraffin single wax-dipping method (Veal et al., 2010; Table S4a,b; Figure S3). Two-way ANOVA was performed in R to statistically compare Symbiodiniaceae cell density and chlorophyll concentration over time between species with Tukey's post-hoc testing upon detecting significance.

2.3 | RNA isolation and sequencing

Frozen coral fragments were immersed in RLT buffer (Qiagen) within zip-lock bags and the tissue was air-picked from the skeleton for a maximum of 3 min. Total RNA was extracted using the Qiagen RNeasy mini kit (Protocol S1). RNA concentrations were assessed using a NanoDrop ND-1000, and RNA quality was evaluated via the presence of intact 18S and 28S ribosomal RNA bands using an Agilent 2100 BioAnalyzer (Agilent Technologies). An Illumina TruSeq RNA prep kit was used to separate the mRNA from the total RNA via polyA selection and to generate 2 × 150bp long paired-end libraries for each sample with an average library size of 364 bp. Sequencing was performed on the Illumina HiSeq 2000 sequencer at the BioScience Core Lab (BCL) at the King Abdullah University of Science and Technology (KAUST).

2.4 | Sequence data processing and analysis

Paired-end reads were quality assessed using FastQC v0.11.5 (Andrews, 1973). Trimmomatic v0.38 (Bolger et al., 2014) was applied to trim off the Illumina adaptors and low-quality regions. Each read was scanned using a 4-base window and cut if the quality of Phred score dropped below 15 (SLIDINGWINDOW:4:15). Leading and trailing bases were removed if quality dropped below a score of 3 (LEADING:3 TRAILING:3). Trimmed reads with resulting lengths shorter than 50 bases were excluded (MINLEN:50). Each sample retained >90% of the paired-end read counts. Trimmed reads were then mapped using Bowtie2 v2.3.5.1 (Langmead & Salzberg, 2012) to the reference genomic gene set (n = 28,188 genes) of *Acropora millepora* (Fuller et al., 2018). Mapping files were processed with SAMtools (Li et al., 2009) for the generation of a bam file and alignment quality check. From the portion of mapped reads, the distribution of mapping quality scores (i.e. the probability of a correct match) and alignment scores (i.e. how similar the sequence read is to the mapping reference) were used to assess mapping performance of the experimental coral species to the reference sequences (Figure S4). Genes that were only mapped by one but not the other experimental coral species ('structural zeros') were removed from downstream analysis (Table S5). Samples with <5 million mapped reads were not considered for downstream analysis. Four *A. selago* samples were removed from downstream analysis: T1 control (×1), T2 treatment (×2) and T3 treatment (×1) (Table S6a,b). Read counts were calculated via eXpress-1.5.1 (Roberts & Pachter, 2013). The batch expectation-maximization algorithm was applied in eXpress to resolve and quantify ambiguously mapped sequence reads. Significantly differentially expressed genes (DEGs; Benjamin-Hochberg, FDR < .05) between treatment and control groups for each time point and coral species were determined using DESeq2 in R (Love et al., 2014). PCA plots for each time point were created using DESeq2 in R. The Gene Ontology (GO) annotations were derived from the EggNOG annotated *A. millepora* genomic gene set. GO enrichment analysis was performed using topGO (Alexa & Rahnenführer, 2019) in R and applied to the set of differentially expressed genes. Annotation of the GO term for 'response to hypoxia' (GO:0001666) was specifically assessed in the DEG lists (Table S11b). KEGG mapper was then used to assess presence of genes for different pathways based on the KEGG Ortholog (KO) annotations from EggNOG with particular focus on the HIF-1 signalling pathway map, KEGG map04066 (Kanehisa & Sato, 2020). FPKM expression estimates were generated via eXpress. Transcripts annotated to the same gene name (e.g. *hsp90*) were pulled together to represent one gene. See Table S7 for KO annotations used for the genes of interest based on the KEGG map04066 and referenced HIF target or stress-associated genes that were used for FPKM analysis over time. RNA-Seq reads from *A. tenuis* and *A. selago* were also mapped to the SymPortal ITS2 reference sequence database (Hume et al., 2019) to assess the putative algal species associated with both coral hosts based on ITS2 type (LaJeunesse et al., 2018).

Data generated from eXpress can be found at the GitHub repository available at https://github.com/reefgenomics/coral_deoxygenation_RNASeq/.

3 | RESULTS

3.1 | Divergent phenotypic response to deoxygenation

Removal of the NTOB resulted in a divergent phenotype for the bleaching-susceptible colony of *A. selago* compared to the bleaching

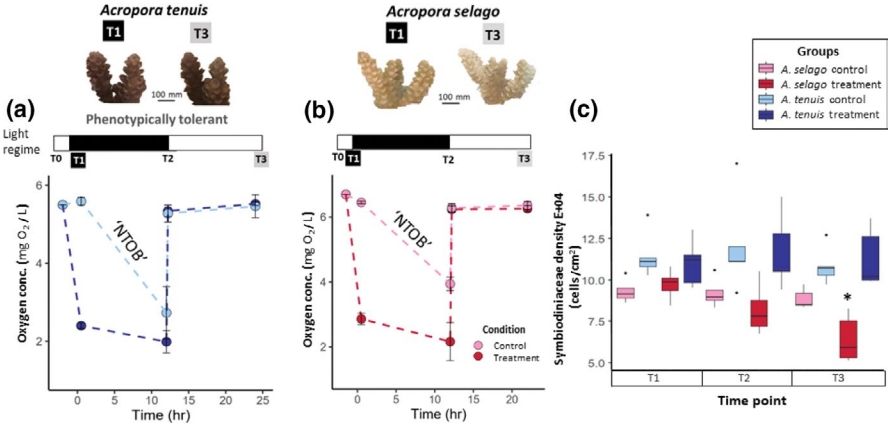

FIGURE 1 Experimental conditions and physiological response of *Acropora tenuis* and *Acropora selago* to hypoxia. (a, b) Oxygen concentration (mg O_2/L) showing removal or maintained 'night-time oxygen buffer' (NTOB), light regime (daylight = white, night-time = black) and typical phenotypes over time points (T) with bars denoting standard error ($n = 5$). (c) Symbiodiniaceae cell density (cells/cm^2) across time points and conditions for both species. Dark pink/blue and light pink/blue indicates treatment and control conditions, respectively, over time points; T1: 0.5 hr, T2: 12 hr, T3: 24 hr. Black dots indicate outliers. Asterisk indicates statistical significance comparing *A. selago* treatment T1 versus T3 ($p < .05$, $n = 8$; T1 vs T3 treatment). Coral replicates per condition group were $n = 5$, except for T1 control and T3 treatment ($n = 4$) and T2 treatment ($n = 3$) for *A. selago* (see main text)

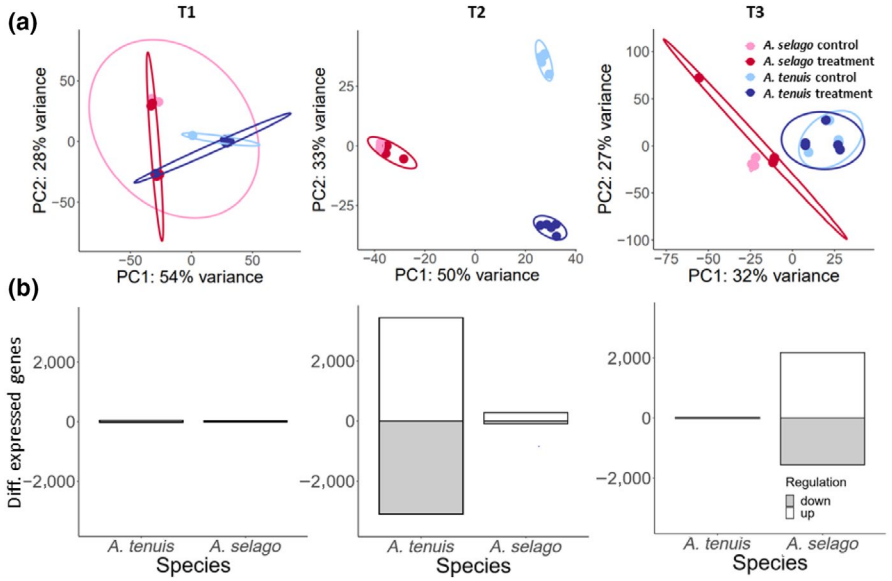

FIGURE 2 Gene expression response of *Acropora tenuis* and *Acropora selago* to deoxygenation. (a) Similarity of samples denoted by principal components analysis for the different time points. Circles denote 95% confidence level of dispersion estimates. (b) Numbers of differentially expressed genes. FDR corrected value ($p_{adj} < .05$) for the different time points. White bars: upregulated genes; grey bars downregulated genes; T1: 0.5 hr, T2: 12 hr, T3: 24 hr. Number of coral replicates per condition group $n = 5$, except for T1 control and T3 treatment ($n = 4$) and T2 treatment ($n = 3$) for *A. selago* (see main text)

resistant *A. tenuis*. Only *A. selago* exhibited onset of a classic bleaching phenotype at T3—loss of Symbiodiniaceae cell content and chlorophyll from the host coral that is well described from heat stress studies (Suggett & Smith, 2020)—whereas *A. tenuis* maintained its original phenotype (Figure 1a,b). Both Symbiodiniaceae cell density and chlorophyll concentration exhibited a significant decline from T1 to T3 for the deoxygenation treatment of *A. selago* but not *A. tenuis* (Figure 1c; $F_{2,1} = 6.7$ and 9.7, respectively $p < .05$; Tables S8 and S9a,b; Figure S5). All control samples for both species remained unimpaired throughout the night to day transition (where NTOB was retained), with no deterioration of the algal symbiosis. In the control samples, *A. tenuis* hosted an overall 26% higher cell density of Symbiodiniaceae than *A. selago* throughout the diel time series (Figure 1c; Table S10a,b). Sequence read mapping to the SymPortal ITS reference sequence database indicated these contrasting hypoxia-driven bleaching responses corresponded with different Symbiodiniaceae associations for the two *Acropora* species, specifically a difference in the dominant species of *Cladocopium* (Figure S6).

3.2 | Contrasting gene expression responses to deoxygenation exposure

To understand the divergent phenotypic response, we evaluated gene expression using RNA-Seq. After exposure to only a short period (0.5 hr) of night-time deoxygenation (T1), gene expression exhibited similarity across experimental conditions and species, with no clear clustering of samples (Figure 2a). Conversely, after 12 hr

of continuous night-time deoxygenation (T2), *A. tenuis* control and treatment samples clustered separately with a high number of differentially expressed genes (DEGs), whereas no apparent differences between *A. selago* samples could be observed by clustering and there were a low number of DEGs (Figure 3b). Finally, after 12 hr reoxygenation (T3), the opposing pattern was observed with separate clusters for *A. selago* control versus treatment, whereas all *A. tenuis* samples clustered together. Notably, the bleaching resistant species, *A. tenuis*, demonstrated a large transcriptional response to deoxygenation exposure while the bleaching-susceptible species, *A. selago*, only exhibited a large response after deoxygenation–re-oxygenation exposure. On average, *A. tenuis* ramped up a greater transcriptional response at earlier time points compared to *A. selago*, with ~18 times more DEGs in *A. tenuis* than in *A. selago* at T2 (6,490 vs. 373 DEGs, respectively; Table S11a). In contrast, *A. tenuis* differentially expressed only two genes by T3 while *A. selago* had 3,737 DEGs. It is possible that this contrasting extent of DEGs for the two species here may partially be influenced by comparing genets (*A. tenuis*) versus clonal ramets (*A. selago*) as we only observe a high number of DEGs at T2 in *A. tenuis*; however, we also observe an equally high number of DEGs expressed in the clonal ramets at T3. Alternately, the gene pattern found for *A. selago* could be explained by the similarity in response to low O_2 by both the control and treatment samples by T2, highlighting a potentially 'delayed' or insufficient response to the deoxygenated conditions for the treatment samples. Gene ontology term for 'response to hypoxia' (GO:0001666) was annotated to only three DEGs when comparing control versus treatment at T2 for *A. selago*, whereas there were 33

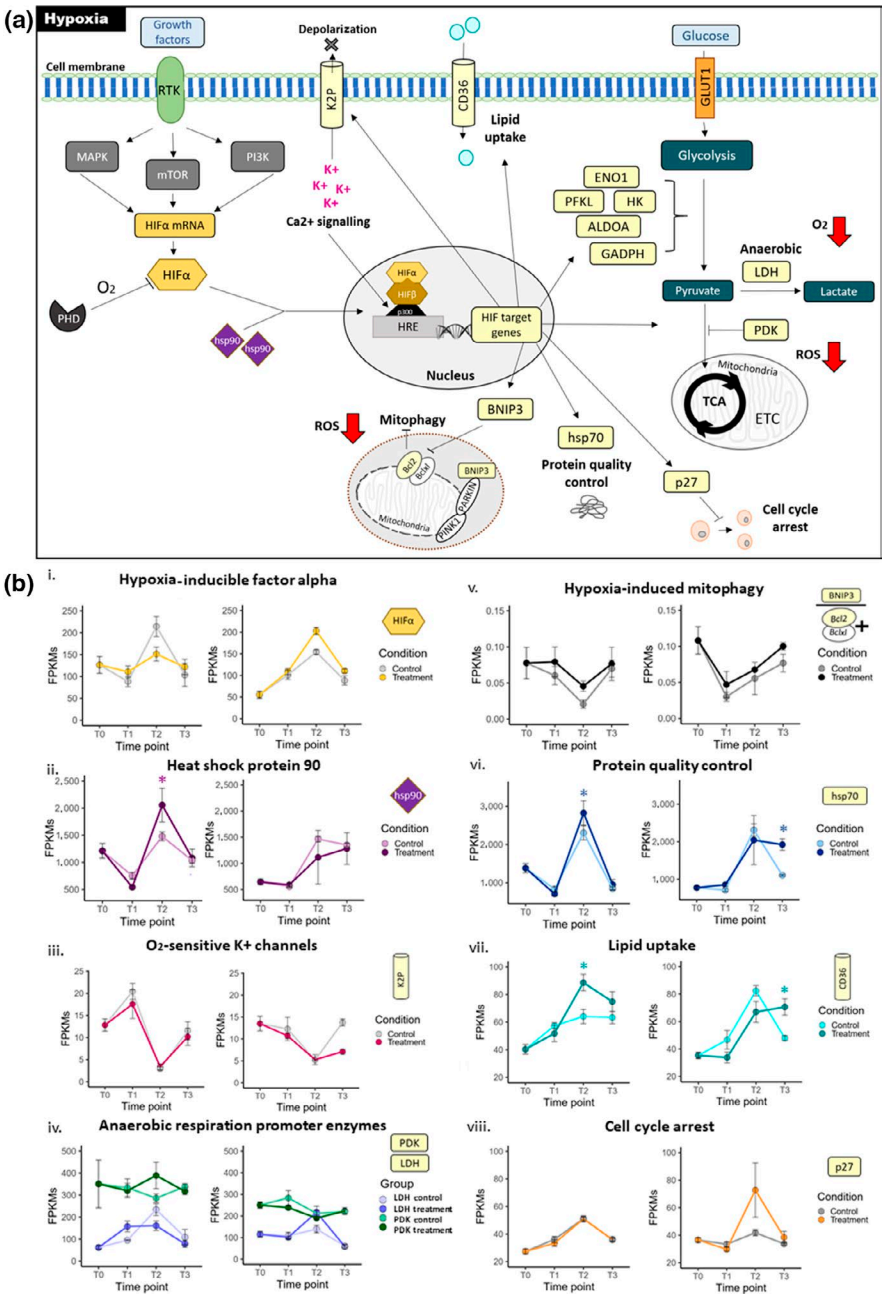

FIGURE 3 Coral HIF pathway and gene expression response to hypoxia. (a) Conceptual model of the coral hypoxia response system (for details on genes refer to the main text). (b) Gene expression dynamics across time points for *Acropora tenuis* (left) and *Acropora selago* (right) for key genes of the HIF system: (i) *HIFα*, (ii) *hsp90AB1/B1*, (iii) oxygen-sensitive K2P potassium ions (TASK-like), (iv) glycolytic enzymes (*LDHA* and *PDK*), (v) hypoxia-induced mitophagy (*BNIP3/Bcl2* + *Bclxl*), (vi) *hsp70*-driven protein quality control, (vii) lipid uptake via scavenger receptor (*CD36*) and (viii) cell cycle arrest (*p27*). FPKM: Fragments per kilobase of transcript per million mapped reads. Asterisk indicates statistical significance following FDR correction, $p < .05$, comparing same time point control and treatment. Error bars denoting standard error with $n = 5$ for each condition group, except for T1 control and T3 treatment ($n = 4$) and T2 treatment ($n = 3$) for *A. selago* (see main text)

DEGs annotated when comparing treatment T1 versus T2, indicating a response to hypoxia at T2 but only to a similar extent as the control samples (Table S11b).

We used KEGG BRITE to functionally interrogate the gene expression responses of both species with specific attention to genes associated with HRS sensitivity (ion channels), metabolic reprogramming (metabolic enzymes) and genetic information processing (e.g. transcription factors, membrane trafficking and DNA repair; Table S12). After 0.5 hr of deoxygenation (T1), only *A. tenuis* exhibited DEGs encoding for 'signalling ion channels' and expressed ~13 times more metabolic enzymes compared to *A. selago* (911 and 75, respectively) after 12 hr of continuous night-time deoxygenation (T2). We observed 10-fold more differentially expressed genes associated with genetic information processing, including genes involved in 'mRNA biogenesis', 'spliceosome', 'chromosome and associated proteins', at T2 for *A. tenuis* compared to *A. selago* (Table S12). Conversely, only by T3 did *A. selago* display its highest number of DEGs encoding for ion channels, metabolic enzymes and genes involved in genetic information processing, suggesting a delayed response to deoxygenation and/or an increased and continuous requirement for transcriptional remodelling even after 12 hr of reoxygenation compared to *A. tenuis* (Table S12).

3.3 | An HRS similar to other metazoans

We annotated the expressed coral genes using the HIF signalling pathway (KEGG map04066) and additionally referenced HIF-associated genes, which revealed that both corals possess a complete HIF pathway from the signalling molecules to the effectors (Figure S7). Based on this, we constructed a conceptual model of coral HRS (Figure 3a) that was subsequently analysed over time to elucidate the mechanistic basis of the coral hypoxia response and gain insight on the HIF transcriptional response to deoxygenation exposure (Figure 3b).

3.4 | Divergent expression of HRS genes

3.4.1 | Hypoxia-inducible factor alpha subunit

Gene expression of *HIFα* 1 hr prior to night-time deoxygenation (T0) in *A. tenuis* was significantly twofold higher than that in *A. selago*, indicative of a greater baseline expression (Figure 3bi; log2 fold change (FC_{log2}) = 1.2, FDR < 0.05; Data S1A). *HIFα* showed dynamic expression over time points for both species with a significant increase in expression from T1 to T2 (*A. tenuis* FC_{log2} = 0.72 and *A. selago* FC_{log2} = 1.02, FDR < 0.05; Data S1A,B), suggesting a strong inducibility and response of this gene to hypoxia, as expected. *HIFα* did not exhibit significant differences between conditions across time points given that control samples also upregulated *HIFα* expression. Both species peaked in *HIFα* expression, across the experimental time points, after 12 hr of night-time deoxygenation (T2). For *A. tenuis*, *HIFα* gene expression was greater after 0.5 hr night-time deoxygenation exposure (T1) but lower after 12 hr (T2) compared to corresponding control samples, which could be indicative of treatment samples peaking in *HIFα* expression earlier in response to reaching cellular hypoxic stress faster. Conversely, we observed similar *HIFα* expression in *A. selago* between treatment and control at T1, while by T2 expression was higher under deoxygenation stress, suggesting a 'delayed' or an extended response to deoxygenation exposure (Figure 3bi). Under the assumption that PHD degradative activity on HIFα is inhibited under hypoxia, we did not focus on the gene expression of PHDs but is reported in Figure S8.

3.4.2 | Heat shock protein 90

Expression of genes encoding for hsp90 (*hsp90AB1* and *hsp90B1*), a protein identified to facilitate the formation of the 'active HIF complex' (Gradin et al., 1996; Hur et al., 2002; Isaacs et al., 2002; Katschinski et al., 2004), followed a pattern similar to HIFα over time points only in *A. tenuis*, with a significant increase from T1 to T2 in treatment samples (*hsp90AB1* FC_{log2} = 2.69 and *hsp90B1* FC_{log2} = 2.02 FDR < 0.05; Data S1A). However, at T2, the expression of *hsp90* had significantly increased under deoxygenation exposure (Figure 3bii; *hsp90AB1* FC_{log2} = 1.08, FDR < 0.05; Data S1A). *hsp90* expression at T2 was twofold higher under deoxygenation exposure in *A. tenuis* compared to *A. selago*, suggesting an increased ability for *A. tenuis* to facilitate formation of the 'active HIF complex' in response to 12 hr of continuous night-time deoxygenation, as well as manage general proteo-toxic stress. Notably, hsp90 encoding genes showed a significantly higher baseline expression of ~twofold (T0) in *A. tenuis* compared to *A. selago* (*hsp90AB1* FC_{log2} = 1.18 and *hsp90B1* FC_{log2} = 0.92, FDR < 0.05; Data S1A), indicative of a greater ability in *A. tenuis* to form active HIF complexes prior to the deoxygenation exposure. Also, in contrast to *A. tenuis*, *hsp90* gene expression remained high or increased even after exposure to 12 hr of reoxygenation (T3) in *A. selago* highlighting possible extension of hsp90-facilitated 'active HIF complex' formation by T3 in attempt to continue utilizing HIF-targeted stress mitigation but also prolonged response to proteo-toxic stress under reoxygenation. Together these data suggest that *A. selago* harbours a lesser ability to ramp its HIF-HRS and sufficiently respond to proteo-toxic stress under deoxygenation–reoxygenation stress.

3.4.3 | HIF target genes

Expression of genes encoding for K2P K^+ ion channels (TASK-like) was consistent over time for both species, irrespective of experimental condition (Figure 3biii). Only *A. tenuis* showed a peak in expression after 0.5 hr of deoxygenation (T1), thus indicating a greater HIF-induced sensitivity in response to short-term deoxygenation (Iorio et al., 2019; Shin et al., 2014). Genes encoding for the glycolytic enzymes lactate dehydrogenase B (*LDH*) and pyruvate dehydrogenase kinase 4 (*PDK*) that are key to promoting anaerobic respiration exhibited dynamic expression changes over time. Most notably, *LDH* expression was observed to increase by T1 under deoxygenation exposure only in *A. tenuis*. Furthermore, *A. tenuis* treatment samples appeared to plateau in

LDH expression by T2, whereas *A. selago* treatment reached a peak in expression at T2 similar to *A. tenuis* under control settings. For *A. tenuis*, genes encoding PDK exhibited a greater expression consistently over all time points and conditions compared to *A. selago*, highlighting a higher baseline level of pyruvate dehydrogenase degradation, reducing the conversion of pyruvate to acetyl-coA and thereby lowering the influx of key acetyl groups into TCA cycle in *A. tenuis* (Figure 3civ). Moreover, *PDK* expression was higher in *A. tenuis* treatment samples than in control samples after 12 hr of deoxygenation (T2) and exhibited a twofold higher expression compared to *A. selago* T2 treatment samples. These expression patterns of *LDH* and *PDK* indicate an earlier and a more substantial shift to anaerobic respiration in *A. tenuis* under deoxygenation exposure.

Hypoxia-induced mitophagy was determined as the ratio of the expression of the pro-apoptosis gene *bnip3* (coding for the Bcl-2 nineteen-kilodalton interacting protein) over the combined expression of the anti-apoptosis genes *bcl2* and *bclxl* (coding for Bcl2 and B-cell lymphoma extra-large, respectively; Pernice et al., 2011; Zhang & Ney, 2009). Only in *A. tenuis* samples under deoxygenation exposure did the mitophagy ratio remain high by T1. Furthermore, the lowest mitophagy ratio for *A. tenuis* was observed at T2 irrespective of condition, while for *A. selago* this occurred at T1 (Figure 3cv), suggesting *A. tenuis* experienced earlier hypoxia stress alleviation via mitophagy compared to *A. selago*. HIF-targeted expression of genes encoding *hsp70*, a protein quality control gene (Honjo et al., 2015), peaked at T2 in *A. tenuis* treatment samples and were differentially expressed by conditions (FC_{log2} = 0.75, 0.32 and 0.78, FDR < 0.05; Data S1A). Whereas *A. selago* exhibited differential expression of *hsp70* encoded genes by T3 with treatment samples higher than control (FC_{log2} = 1.81, 0.35, 2.07 and 1.80, FDR < 0.05; Data S1B), suggesting a greater extent of proteo-toxic stress management in response to 12 hr of continuous deoxygenation exposure in *A. tenuis*.

The scavenger receptor, CD36, uptakes lipids for cellular energy use and oxidized lipids to be degraded (Febbraio & Silverstein, 2009). *CD36* gene expression increases by T1 only in *A. tenuis*, implying an earlier promotion of lipid uptake (Figure 3cvii). Furthermore, *CD36* expression peaked and was differentially expressed by conditions at T2 for *A. tenuis* only, as *A. selago* treatment samples exhibited highest *CD36* expression by T3 with differential expression between conditions, indicating lipid uptake to continue increasing only in *A. selago* even after 12 hr of reoxygenation (FC_{log2} = 0.60 and 0.93, FDR < 0.05, respectively; Data S1A,B). Finally, the expression of the cell cycle arrest gene *p27* peaked at T2 for both species irrespective of condition. However, at this time point *p27* expression levels for *A. selago* were greater in treatment samples compared to control, suggesting a greater extent in arrest of cell cycling, possibly for a more 'extreme' means of cellular protection by preventing new cells from damage (Figure 3bvii).

3.5 | Divergent hypoxia-induced stress response

Finally, to assess processes driving bleaching of the *A. selago* coral replicates but not those of *A. tenuis*, we examined genes indicative of hypoxia-induced stress responses and HIF-HRS functioning (Figure 4). This section considers genes involved in regulating mitochondrial

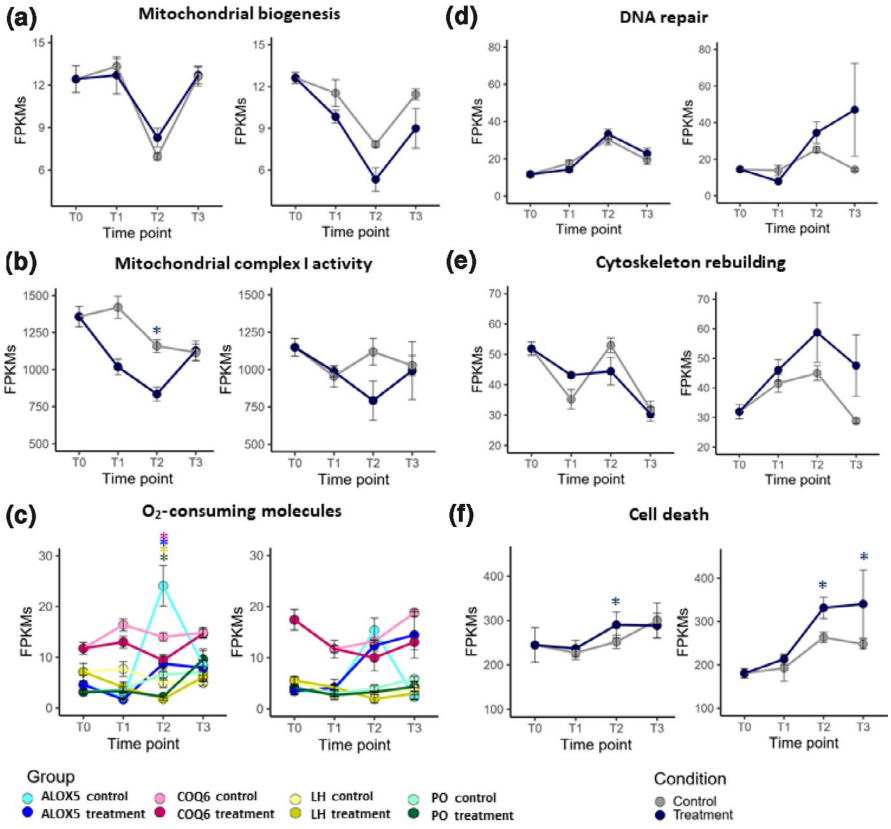

FIGURE 4 Hypoxia-induced stress response of *Acropora tenuis* and *Acropora selago* (left and right graph in each panel, respectively). Expression of the following genes associated with stress in coral: (a) RNA Polymerase Mitochondrial (*POLRMT*), (b) NADPH dehydrogenase (*NDUF*), (c) O_2-consuming molecules (arachidonate lipoxygenase; *ALOX5*), Coenzyme Q6 monooxygenase (*COQ6*), lactase hydrolase (*LH*) and polyamine oxidase (*PO*), (d) Growth Arrest and DNA Damage (*GADD45*), (e) actin beta/gamma (*ACTBG1*), and (f) terminal cell death protease (*Casp3*). FPKM, fragments per kilobase of transcript per million mapped reads. Asterisk indicates statistical significance following FDR correction, $p < .05$, comparing same time point control and treatment. Error bars denoting standard error with $n = 5$ for each condition group, except for T1 control and T3 treatment ($n = 4$) and T2 treatment ($n = 3$) for *A. selago* (see main text)

biogenesis (*POLRMT*) and complex activity (*NADPH dehydrogenase*), DNA repair (*GADD45*), cytoskeleton repair (*Actin gamma*), cell death (*casp3*), as well as genes coding for molecules that consume O_2.

POLMRT expression in *A. tenuis* declined at T2 irrespective of condition, implying a reduction in mitochondrial formation as a more 'extreme' means of protecting cells from ROS-derived stress under hypoxic conditions when mitophagy is not sufficient. In contrast, *POLRMT* expression declined at both T1 and T2 in *A. selago* and was notably lower for treatment samples compared to control over time points 1–3, suggesting a greater and earlier reduction in mitochondrial formation for *A. selago* compared to *A. tenuis* (Figure 4a). Expression of *NADPH dehydrogenase* (coding for a key enzyme regulating the influx of NADPH-sourced electrons to the mitochondrial complex I) decreased from T0 to T2 in both species' and treatment groups (Figure 4b). This indicates a reduced mitochondrial complex I activity in response to increased deoxygenation exposure and may reflect both the lower mass and activity of mitochondria implemented by HIF under hypoxia. Furthermore, genes encoding *NADPH dehydrogenase* were differentially expressed in *A. tenuis* between conditions at T2 (FC_{log2} = −0.55, −0.60, −0.41 and −0.54, FDR < 0.05; Data S1A). We only observed differential expression of genes encoding O_2-consuming molecules (arachidonate lipoxygenase, monooxygenase, lactase hydrolase and polyamine oxidase) in *A. tenuis* between conditions at T2, where treatment samples showed lower expression levels than control (FC_{log2} = −1.36, −0.50, −1.36 and −1.47, FDR < 0.05, respectively; Data S1A). This indicates that *A. tenuis* might have experienced a decline in O_2-consuming reactions in response to night-time deoxygenation (Figure 4c).

The expression of the gene *GADD45* (involved in growth arrest and DNA damage), an indicator of DNA repair, remained largely constant across time points between conditions for *A. tenuis*. By contrast, *GADD45* expression in *A. selago* under deoxygenation was twofold higher compared to control samples at T3, indicating an increase in DNA damage and repair after night-time deoxygenation and subsequent daytime reoxygenation (Figure 4d). The actin gamma gene *ACTGB1* (involved in cytoskeleton rebuilding) exhibited a greater expression in *A. selago* treatment compared to control settings at T2 and T3, indicating an increase in cytoskeleton repair in response to deoxygenation exposure but possibly also a roll-on-effect of the induced stress to T3 (Figure 4e).

Finally, the *casp3* gene (encoding the terminal protease for cell death) exhibited a similar expression pattern to *actin gamma* in *A. selago* (Figure 4e,f). *casp3* expression was greater under treatment settings at T2 and T3 compared to control, with differential expression between conditions at T3 (FC_{log2} = 0.40, FDR < 0.05; Data S1B). Furthermore, *A. tenuis* also differentially expressed *casp3* between conditions at T2 with greater expression in treatment compared to control (FC_{log2} = 0.65, FDR < 0.05; Data S1A). This expression pattern of *casp3* suggests that only *A. selago* increased cell death in response to the deoxygenation and subsequent reoxygenation phases of the experiment, thereby reinforcing reduced ability to return to 'normal' state.

4 | DISCUSSION

O_2 availability has recently been highlighted as a critical but overlooked factor in affecting the susceptibility of coral to bleaching (Hughes et al., 2020; Suggett & Smith, 2020), and thus governing how corals will survive under climate change where reef waters are subject to parallel warming and deoxygenation (Altieri et al., 2017; Hughes et al., 2020). In the present study, we explored (a) the fundamental cellular mechanisms employed by *A. tenuis* to cope with the large daily oscillations in O_2 availability and (b) whether the management of their night-time intracellular hypoxic state has the capacity to also support their cellular O_2 requirements when under further deoxygenation by removal of their NTOB. We discovered that corals possess a complete and active HIF-mediated HRS homologous to other metazoans. To determine how this observation applies to other corals, we exposed replicate fragments from a single *A. selago* (stress-susceptible) colony to the same experimental design to specifically examine for any deviations to the HIF-driven stress regulation found in the more stress-resistant *Acropora tenuis* species. As expected, *A. selago*, but not *A. tenuis*, exhibited a visible stress phenotype (bleaching) to a reduced O_2 environment. These divergent bleaching phenotypes aligned to differences in baseline expression of *HIFα* prior to stress exposure, the extent of *HIFα* expression by the end of deoxygenation stress (e.g. reflecting an ability to downregulate *HIFα* under low O_2) and the expression of HIF-dependent *hsp90*, which we suggest affected the effectiveness of the HIF response. Together, these findings suggest that corals can vary in their capacity to facilitate extended cellular metabolic reprogramming and damage control in response to stress imposed by strong deoxygenation.

Only *A. selago* exhibited a bleaching phenotype under NTOB removal after a single night–day cycle. In contrast, *A. tenuis* maintained its original phenotype throughout the experiment. These observed differences aligned with underlying differences in gene expression (Figure 2a). Only *A. tenuis* exhibited a clear clustering of control and treatment samples after 12 hr of continuous deoxygenation during the night-time (T2), followed by convergence of gene expression profiles between control and treatment samples after 12 hr of daylight reoxygenation (T3), as indicated by their clustering. Such gene divergence and subsequent convergence patterns infer 'transcriptome resilience', whereby the organism can successfully ramp a gene expression response to meet the altered metabolic states but returns back to 'normal' functioning upon cessation of the stressor (sensu *Acropora hyacinthus*; Seneca & Palumbi, 2015).

Differences in DEGs between treatment and control at T2 for *A. tenuis* indicated a reduction in transcribed O_2-consuming reactions (e.g. involving monooxygenases) and mitochondrial activity, while an increase in genetic information processing genes (such as retrotransposons and tandem repeats, i.e. armadillo repeats) highlighted the different molecular levels in which the removal of their NTOB could have been tolerated (Data S2A). In contrast, *A. selago* exhibited the largest response by means of DEGs at T3 inferring inferior capacity to deal with loss of their NTOB or a delayed response to low O_2-induced stress (Figure 2b). Furthermore, DEGs associated with cell stress,

damage and death (e.g. Death Domain including Ankyrin repeats) were only observed for *A. selago* when at T3, indicating the transition to a bleaching-susceptible state during their photosynthetically active period between T2 and T3 (Data S2B). This is consistent with the proposed bleaching trigger sequence of photo-oxidative stress reaching lethal capacity after a stress event (Cziesielski et al., 2019; Downs et al., 2013; Weis, 2008), in this case post-deoxygenation stress. So, how do these corals respond to deoxygenation stress and what attributes appear to regulate their different hypoxia tolerance?

While being closely related to the most primitive metazoans, Porifera (i.e. sponges) that lack key HIF system components (Mills et al., 2018), corals have a complete and functional HRS similar to other metazoans. We propose the first conceptual model for the mechanistic basis of the coral hypoxia response (Figure 3a) based on the presence of genes from the mammalian HIF signalling pathway, but also involving HIF interactive molecules such as heat shock proteins, which we explicitly considered and integrated, given high prevalence of their upregulation in thermally stressed corals (Bellantuono et al., 2012; Desalvo et al., 2010; Gates & Edmunds, 1999; Kenkel et al., 2013).

The conceptual model allowed us to query the expression of key genes over time, which highlighted several key characteristics: First, a significant increase in *HIFα* expression with increasing deoxygenation exposure for both *Acropora* species, and for both control and treatment corals throughout the night. However, *A. tenuis* showed higher *HIFα* expression at T1 and lower at T2 in treatment samples compared to controls indicative of an earlier induction and peak in response to cellular hypoxia stress under 12 hr of continuous deoxygenation. *HIFα* expression from the *A. tenuis* treatment samples exemplifies the importance of *HIFα* downregulation during low O_2 conditions as a means to prevent harmful prolonged high expression levels or simply reflecting a more sufficient adjustment in response to hypoxia. Furthermore, *HIFα* expression in *A. selago* was lower under control settings at T2 compared to *A. tenuis* suggesting a decreased induction of *HIFα* expression in response to cellular hypoxia stress. As well as emphasizing the intracellular hypoxic state experienced by the coral during night-time, our results also infer that *A. selago* experiences lower night-time hypoxia stress. This could be a consequence of lower cell densities of Symbiodiniaceae and so less dramatic night-time deoxygenation (Figure 1c), different populations of microbes (microalgae, bacteria, fungi or archaea) with alternate O_2 metabolism (Ziegler et al., 2017) or differences in host basal metabolism (Camp et al., 2017).

Second, *hsp90* expression increased under intensified deoxygenation stress and under continuous *HIFα* expression in both coral species. Not only did *A. tenuis* treatment samples show a greater *hsp90* expression at T2 compared to *A. selago*, but *A. selago* treatment samples showed lower *hsp90* expression compared to control settings implying a lesser ability to facilitate active 'HIF complex' formation in *A. selago* in response to cellular hypoxia during night-time. Alternate bleaching phenotypes could thus be a product of *hsp90* gene expression capping the transcriptional activation of their HIF-HRS as well as management of general proteo-toxic stress. Furthermore, this study may also support the proposed function of HIF-targeted *hsp70* to also regulate HIFα protein levels by degrading HIFα when the HIF system has sufficiently responded but reoxygenation has yet to have occurred (Luo et al., 2010). This can be exemplified by *A. tenuis* as *HIFα* expression may already have peaked before T2 and so *hsp70* could also be functioning to degrade HIFα, to prevent any unnecessary and detrimental HIFα expression and thereby acting in an internalized negative feedback loop in the absence of O_2. We propose that *A. selago* achieved less active 'HIF complexes' due to relatively lower *hsp90* expression and thereby expressed lower levels of HIF-targeted *hsp70*. The lower HIF-targeted gene network in *A. selago* may then have also delayed the need of the secondary function of hsp70 as part of an internalized negative feedback loop of HIFα. Overall, our finding of higher expression of both *hsp90* and *hsp70* is consistent with previous reports of higher expression of these genes in stress-tolerant corals (Franzellitti et al., 2018; Poli et al., 2017; Seveso et al., 2018). Most importantly, *A. tenuis* demonstrated a greater ability to upregulate and downregulate HIFα implying a more finely tuned regulation of the HIF system, which facilitates a more rapid adjustment to the low oxygen environment, and a response consistent in hypoxia tolerance in other metazoans where HIF stress responses become suppressed during prolonged hypoxia exposure, for example, in high altitudes (Peng et al., 2017).

Third, *A. tenuis* deployed a more regulated systemic response, by which the HIF-targeted genes could effectively manage the deoxygenation–reoxygenation exposure compared to *A. selago*. HIF-targeted K2P genes (TASK-like, encoding for two-pore domain potassium ion channels) exhibited a peak in expression at T1 for only *A. tenuis*. Potassium ions are known to act as 'detectors' of cellular O_2 changes in metazoans, thus greater expression of these potassium ion channels in response to deoxygenation is consistent with the notion of a more sensitive HIF-HRS for *A. tenuis* (López-Barneo et al., 2001; Wang et al., 2017). The HIF-associated metabolic reprogramming and mitochondrial quality control were more evident in *A. tenuis*. A critical metabolic shift to anaerobic respiration in *A. tenuis* when faced with limited cellular O_2 was indicated by an increased expression of *LDH* after 0.5 hr deoxygenation exposure (T1) and increased *PDK* expression with continued deoxygenation (T2). In contrast, *LDH* expression in *A. selago* did not show an increase until T2 and *PDK* expression remained relatively constant implying a delay and/or an absence of a pivotal metabolic transition in response to deoxygenation. Interestingly, an increase in mitochondrial ROS has also been observed to accompany hypoxia (Chandel et al., 2000) potentially resulting in mitochondrial degradation (Dunn et al., 2012). Furthermore, high levels of Symbiodiniaceae-associated ROS are widely acknowledged as a core attributing factor to bleaching of corals under thermal stress (Suggett & Smith, 2020; Weis, 2008). Alongside a network of antioxidants, a strategy to combat high ROS levels in mammalian cells is to activate mitophagy to directly remove the main producer of ROS, that is, mitochondria. In agreement, hypoxia-induced mitophagy appeared to occur in *A. tenuis* at the onset of deoxygenation exposure (T1) but was then reduced following prolonged exposure (T2). While *A. selago* only appeared to increase hypoxia-induced mitophagy from T1 to T2. Corals may thus utilize mitophagy to remove unused, damaged or misfunctioning

mitochondria under oxidative and hypoxic stress when anaerobic respiration (e.g. indicated via *LDH* expression) is not yet sufficient.

The commonly expressed hsp gene involved in protein quality control, *hsp70*, is also described as a HIF-target gene (Honjo et al., 2015) along with the *CD36* gene involved in lipid scavenging. The expression of both genes peaked after continued deoxygenation (T2) in *A. tenuis* but remained highly expressed by T3 in *A. selago*, indicative of high protein and lipid stress in response to 12 hr deoxygenation and subsequent 12 hr reoxygenation in this coral species. Importantly, only *A. tenuis* demonstrated an early increase in *CD36* expression (T1). Furthermore, the gene encoding for hypoxia stress-induced cell cycle arrest, *p27* was more highly expressed in *A. selago* after night-time deoxygenation indicative of a more 'extreme' stress-mitigating mechanism implemented to manage hypoxia stress by T2 in *A. selago*. Our results suggest the phenotypically tolerant *A. tenuis* can employ HIF-regulated hypoxia stress 'counter-measures' more quickly and more effectively, compared to the phenotypically susceptible *A. selago*.

Finally, the inducibility of the HIF-HRS between coral species was further reinforced by the observed temporal changes in expression of different coral stress genes. Most notably, only treatment samples for *A. selago* exhibited increased and sustained gene expression of the *Actin gamma* gene previously reported to be involved in coral cytoskeleton rebuilding (DeSalvo et al., 2008), the *GADD45* gene involved in DNA repair (Liew et al., 2018), and the *Casp3* gene involved in terminal cell death (Pernice et al., 2011) in response to 12 hr continuous deoxygenation and subsequent 12 hr reoxygenation exposure. Interestingly, *A. tenuis* exhibited a greater initial expression of *Casp3* than *A. selago*, and such higher cell death cycling—especially under early stress—could potentially contribute to a more effectively stress-resistant phenotype (Ainsworth et al., 2011). Moreover, a mitochondrial biogenesis regulating enzyme (POLRMT) appeared to cease expression during T2 for both species, possibly reflecting the damaging or redundant actions of mitochondrial replacement given mitochondrial oxidative stress levels and diversion of the respiratory pathway from the mitochondria to only the cytosol (anaerobic) in response to such a hypoxic environment (Scarpulla et al., 2012). Lastly, gene expressions of O_2-consuming molecules (e.g. arachidonate lipoxygenase) were found to decrease under treatment relative to control settings only in *A. tenuis* after 12 hr of continuous deoxygenation exposure indicating an additional means of shifting the dependency on cellular O_2 to compensate while under hypoxia stress.

In summary, we present the first conceptual model of the coral HRS and highlight the key attributes found to differ in *Acropora* species with different bleaching phenotypes, which appear to potentiate or limit their success in responding to deoxygenation-driven hypoxia stress (Figure 5). We propose that the bleaching-tolerant coral had

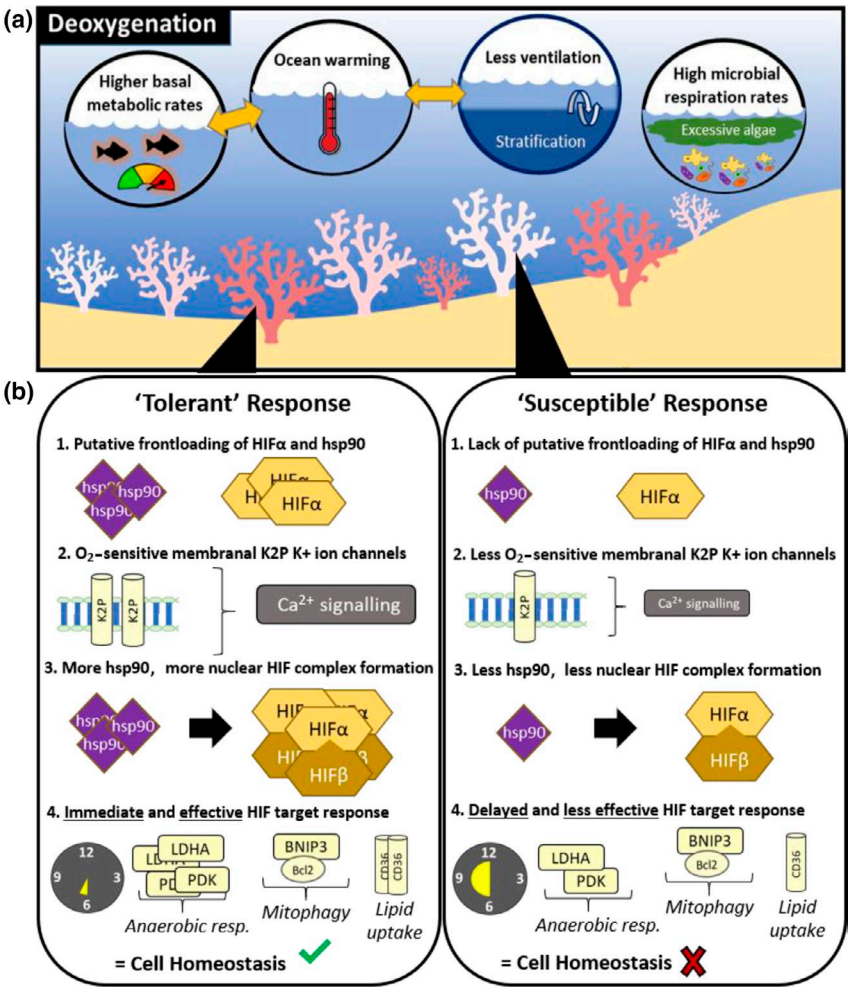

FIGURE 5 Differences in coral hypoxia response system (HRS) that could determine bleaching susceptibility. (a) Schematic of environmental factors contributing to the deoxygenation of coral reef water bodies; higher basal metabolic rates, ocean warming, less ocean ventilation and high eutrophication-driven microbial respiration. Orange arrows indicate interactive effects. Colour gradient of coral from darker pink to white indicates coral hypoxia tolerance variance. (b) The key attributes of the HIF-HRS found to differ in 'tolerant' and 'susceptible' bleaching phenotypes framed in this study in response to deoxygenation stress

an effective HRS to lowered O_2 conditions (removed NTOB) and re-oxygenation, sustained through greater baseline expression of *HIFα* and HIF-dependent *hsp90* to rapidly coordinate O_2-detecting potassium ion channels, a metabolic shift reducing mitochondrial aerobic activity, efficient use of mitophagy, enhanced protein quality control and lipid uptake, and finely regulated cell cycle and death. However, most importantly, low O_2 tolerance could be driven by the ability to both upregulate and downregulate *HIFα* under low O_2 conditions (e.g. via *hsp70*-dependent *HIFα* degradation) due to the detrimental metabolic depression that threatens cell survival during long periods of high HIFα expression and HIF system activation. Therefore, there is likely a threshold to what is a 'beneficial' baseline expression of *HIFα*. Given how interlinked cellular management of hypoxia and oxidative stress appear to be in corals, and how the 'Oxidative Stress Theory' persists in current coral bleaching models (Cziesielski et al., 2019; Downs et al., 2002), these key attributes of the HRS may also point to a more fundamental metabolic basis of what drives coral susceptibility to stress-induced bleaching (Cziesielski et al., 2019; Suggett & Smith, 2020; Weis, 2008). However, detailed assessment across coral species and populations will be required to verify whether and how HIF-HRS shape could shape variation in bleaching susceptibility. It will be particularly critical to ascertain how such metabolic pathways manifest across the multiple stressors (e.g. high temperature-low O_2), which potentially co-regulate—and thus ultimately cross talk—via mutual effects on HIF-HRS. Identifying such 'common switch' repertoires to stress may, in turn, provide novel means to identify genes of interest for coral management or as targets for genetic modification or selection (Anthony et al., 2017). Resolving how the HIF-HRS response may govern coral survival under RCP emission scenarios that concurrently drive widespread ocean warming and deoxygenation will be a critical step towards this goal.

ACKNOWLEDGEMENTS

We wish to particularly thank teams from James Cook University Cairns (led by Jamie Seymour, Katie Chartrand) and Southern Cross University (led by Peter Harrison, Nadine Boulotte) for their invaluable support in collecting corals used in this study (Vlasoff Reef, northern Great Barrier Reef) and subsequent holding in large-scale acclimation aquaria prior to experimentation. All corals were collected under a Great Barrier Reef Marine Park Zoning Plan 2003 Part 5.4 Authorization (MPA18/002 'Coral larval restoration and Symbiodinium co-culture collaborative project') to Peter Harrison. Also, immense thanks to the King Abdullah University of Science and Technology's Bioscience Core Lab (BCL) for assistance with Illumina sequencing. Funding for this work was supported by an Australian Research Council (ARC) Discovery Grant (DP180100074) to D.J.S., M.P., M.K. and C.R.V. M.K. acknowledges support by the Gordon and Betty Moore Foundation (grant number GBMF9206, https://doi.org/10.37807/GBMF9206). C.R.V. acknowledges support by the Deutsche Forschungsgemeinschaft (DFG, German Research Foundation) project number 433042944. Open access funding enabled and organized by Projekt DEAL. [Correction added on 19 November 2020, after first online publication: Projekt Deal funding statement has been added.]

CONFLICT OF INTEREST

The authors declare no competing interests.

AUTHOR CONTRIBUTION

D.J.S., M.P., C.R.V., M.K., D.J.H. and R.A. designed and conceived the experiment; D.J.H. and R.A. collected the samples and conducted the experiment; R.A. processed all the sample types; A.C. generated the sequencing library preparations; C.R.V., A.C. and R.A. analysed the RNA-Seq data; R.A. conducted the statistics and generated figures; R.A., D.J.S. and C.R.V. wrote the paper with input from all authors. All authors reviewed and approved the final manuscript.

DATA AVAILABILITY STATEMENT

Sequence data determined in this study are available at https://www.ncbi.nlm.nih.gov/bioproject/PRJNA635763. Source data underlying figures and statistical analyses are provided in the supplementary material. Scripts used in RNA-Seq data analysis pipeline can be found at the GitHub repository available at https://github.com/reefgenomics/coral_deoxygenation_RNASeq/.

ORCID

Rachel Alderdice https://orcid.org/0000-0002-4234-7673
David J. Suggett https://orcid.org/0000-0001-5326-2520
Anny Cárdenas https://orcid.org/0000-0002-4080-9010
David J. Hughes https://orcid.org/0000-0003-3778-7460
Michael Kühl https://orcid.org/0000-0002-1792-4790
Mathieu Pernice https://orcid.org/0000-0002-3431-2104
Christian R. Voolstra https://orcid.org/0000-0003-4555-3795

REFERENCES

Ainsworth, T. D., Wasmund, K., Ukani, L., Seneca, F., Yellowlees, D., Miller, D., & Leggat, W. (2011). Defining the tipping point. A complex cellular life/death balance in corals in response to stress. *Scientific Reports*, *1*(1). https://doi.org/10.1038/srep00160

Alexa, A., & Rahnenführer, J. (2019). *Gene set enrichment analysis with topGO*. http://www.mpi-sb.mpg.de/~alexa

Altieri, A. H., Harrison, S. B., Seemann, J., Collin, R., Diaz, R. J., & Knowlton, N. (2017). Tropical dead zones and mass mortalities on coral reefs. *Proceedings of the National Academy of Sciences of the United States of America*, *114*(14), 3660–3665. https://doi.org/10.1073/pnas.1621517114

Andrews, S. (1973). Babraham Bioinformatics – FastQC a quality control tool for high throughput sequence data. https://doi.org/10.1016/0038-0717(73)90093-X

Anthony, K., Bay, L. K., Costanza, R., Firn, J., Gunn, J., Harrison, P., Heyward, A., Lundgren, P., Mead, D., Moore, T., Mumby, P. J., van Oppen, M. J. H., Robertson, J., Runge, M. C., Suggett, D. J., Schaffelke, B., Wachenfeld, D., & Walshe, T. (2017). New interventions are needed to save coral reefs. *Nature Ecology & Evolution*, *1*(10), 1420–1422. https://doi.org/10.1038/s41559-017-0313-5

Bellantuono, A. J., Granados-Cifuentes, C., Miller, D. J., Hoegh-Guldberg, O., & Rodriguez-Lanetty, M. (2012). Coral thermal tolerance: Tuning gene expression to resist thermal stress. *PLoS ONE*, *7*(11), e50685. https://doi.org/10.1371/journal.pone.0050685

Benita, Y., Kikuchi, H., Smith, A. D., Zhang, M. Q., Chung, D. C., & Xavier, R. J. (2009). An integrative genomics approach identifies Hypoxia Inducible Factor-1 (HIF-1)-target genes that form the core response

to hypoxia. *Nucleic Acids Research*, *37*(14), 4587–4602. https://doi.org/10.1093/nar/gkp425

Bernasconi, R., Stat, M., Koenders, A., Paparini, A., Bunce, M., & Huggett, M. J. (2019). Establishment of coral-bacteria symbioses reveal changes in the core bacterial community with host ontogeny. *Frontiers in Microbiology*, *10*, 1529. https://doi.org/10.3389/fmicb.2019.01529

Blokhina, O., Virolainen, E., & Fagerstedt, K. V. (2003). Antioxidants, oxidative damage and oxygen deprivation stress: A review. *Annals of Botany*, *91*(2), 179–194. https://doi.org/10.1093/aob/mcf118

Bolger, A. M., Lohse, M., & Usadel, B. (2014). Trimmomatic: A flexible trimmer for Illumina sequence data. *Bioinformatics*, *30*(15), 2114–2120. https://doi.org/10.1093/bioinformatics/btu170

Breitburg, D., Levin, L. A., Oschlies, A., Grégoire, M., Chavez, F. P., Conley, D. J., Garçon, V., Gilbert, D., Gutiérrez, D., Isensee, K., Jacinto, G. S., Limburg, K. E., Montes, I., Naqvi, S. W. A., Pitcher, G. C., Rabalais, N. N., Roman, M. R., Rose, K. A., Seibel, B. A., … Zhang, J. (2018). Declining oxygen in the global ocean and coastal waters. *Science*, *359*(6371), eaam7240. https://doi.org/10.1126/science.aam7240

Bruick, R. K., & McKnight, S. L. (2001). A conserved family of prolyl-4-hydroxylases that modify HIF. *Science*, *294*(5545), 1337–1340. https://doi.org/10.1126/science.1066373

Camp, E. F., Edmondson, J., Doheny, A., Rumney, J., Grima, A. J., Huete, A., & Suggett, D. J. (2019). Mangrove lagoons of the Great Barrier Reef support coral populations persisting under extreme environmental conditions. *Marine Ecology Progress Series*, *625*, 1–14. https://doi.org/10.3354/meps13073

Camp, E. F., Krause, S.-L., Santos, L. M. F., Naumann, M. S., Kikuchi, R. K. P., Smith, D. J., Wild, C., & Suggett, D. J. (2015). The "Flexi-Chamber": A novel cost-effective in situ respirometry chamber for coral physiological measurements. *PLoS One*, *10*(10), e0138800. https://doi.org/10.1371/journal.pone.0138800

Camp, E. F., Nitschke, M. R., Rodolfo-Metalpa, R., Houlbreque, F., Gardner, S. G., Smith, D. J., Zampighi, M., & Suggett, D. J. (2017). Reef-building corals thrive within hot-acidified and deoxygenated waters. *Scientific Reports*, *7*(1), 1–9. https://doi.org/10.1038/s41598-017-02383-y

Chandel, N. S., McClintock, D. S., Feliciano, C. E., Wood, T. M., Melendez, J. A., Rodriguez, A. M., & Schumacker, P. T. (2000). Reactive oxygen species generated at mitochondrial complex III stabilize hypoxia-inducible factor-1α during hypoxia: A mechanism of O_2 sensing. *Journal of Biological Chemistry*, *275*(33), 25130–25138. https://doi.org/10.1074/jbc.M001914200

Cziesielski, M. J., Schmidt-Roach, S., & Aranda, M. (2019). The past, present, and future of coral heat stress studies. *Ecology and Evolution*, *9*(17), 10055–10066. https://doi.org/10.1002/ece3.5576

Dengler, V. L., Galbraith, M. D., & Espinosa, J. M. (2014). Transcriptional regulation by hypoxia inducible factors. *Critical Reviews in Biochemistry and Molecular Biology*, *49*(1), 1–15. https://doi.org/10.3109/10409238.2013.838205

DeSalvo, M. K., Voolstra, C. R., Sunagawa, S., Schwarz, J. A., Stillman, J. H., Coffroth, M. A., Szmant, A. M., & Medina, M. (2008). Differential gene expression during thermal stress and bleaching in the Caribbean coral *Montastraea faveolata*. *Molecular Ecology*, *17*(17), 3952–3971. https://doi.org/10.1111/j.1365-294X.2008.03879.x

DeSalvo, M. K., Estrada, A., Sunagawa, S., & Medina, M. (2012). Transcriptomic responses to darkness stress point to common coral bleaching mechanisms. *Coral Reefs*, *31*(1), 215–228. https://doi.org/10.1007/s00338-011-0833-4

DeSalvo, M. K., Sunagawa, S., Voolstra, C. R., & Medina, M. (2010). Transcriptomic responses to heat stress and bleaching in the Elkhorn coral *Acropora palmata*. *Marine Ecology Progress Series*, *402*, 97–113. https://doi.org/10.3354/meps08372

Downs, C. A., Fauth, J. E., Halas, J. C., Dustan, P., Bemiss, J., & Woodley, C. M. (2002). Oxidative stress and seasonal coral bleaching. *Free Radical Biology and Medicine*, *33*(4), 533–543. https://doi.org/10.1016/S0891-5849(02)00907-3

Downs, C. A., McDougall, K. E., Woodley, C. M., Fauth, J. E., Richmond, R. H., Kushmaro, A., Gibb, S. W., Loya, Y., Ostrander, G. K., & Kramarsky-Winter, E. (2013). Heat-stress and light-stress induce different cellular pathologies in the symbiotic dinoflagellate during coral bleaching. *PLoS One*, *8*(12), e77173. https://doi.org/10.1371/journal.pone.0077173

Dunn, S. R., Pernice, M., Green, K., Hoegh-Guldberg, O., & Dove, S. G. (2012). Thermal stress promotes host mitochondrial degradation in symbiotic cnidarians: Are the batteries of the reef going to run out? *PLoS One*, *7*(7), e39024. https://doi.org/10.1371/journal.pone.0039024

Febbraio, M., & Silverstein, R. (2009). CD36, a scavenger receptor involved in immunity, metabolism, angiogenesis, and behavior. *Science Signalling*, *2*(72), re3. https://doi.org/10.1126/scisignal.272re3

Franzellitti, S., Airi, V., Calbucci, D., Caroselli, E., Prada, F., Voolstra, C. R., Mass, T., Falini, G., Fabbri, E., & Goffredo, S. (2018). Transcriptional response of the heat shock gene hsp70 aligns with differences in stress susceptibility of shallow-water corals from the Mediterranean Sea. *Marine Environmental Research*, *140*, 444–454. https://doi.org/10.1016/j.marenvres.2018.07.006

Fuller, Z. L., Liao, Y. I., Bay, L., Matz, M., & Przeworski, M. (2018). *Acropora millepora genome assembly*. https://github.com/wtsi-hpag/Scaff10X

Gabaldón, T., & Pittis, A. A. (2015). Origin and evolution of metabolic sub-cellular compartmentalization in eukaryotes. *Biochimie*, *119*, 262–268. https://doi.org/10.1016/j.biochi.2015.03.021

Gates, R. D., & Edmunds, P. J. (1999). The physiological mechanisms of acclimatization in tropical reef corals. *American Zoologist*, *39*, 30–43. https://doi.org/10.1093/icb/39.1.30

Glück, A. A., Aebersold, D. M., Zimmer, Y., & Medová, M. (2015). Interplay between receptor tyrosine kinases and hypoxia signaling in cancer. *International Journal of Biochemistry and Cell Biology*, 101–114. https://doi.org/10.1016/j.biocel.2015.02.018

Gradin, K., McGuire, J., Wenger, R. H., Kvietikova, I., fhitelaw, M. L., Toftgård, R., Tora, L., Gassmann, M., & Poellinger, L. (1996). Functional interference between hypoxia and dioxin signal transduction pathways: Competition for recruitment of the Arnt transcription factor. *Molecular and Cellular Biology*, *16*(10), 5221–5231. https://doi.org/10.1128/mcb.16.10.5221

Graham, A. M., & Barreto, F. S. (2019). Loss of the HIF pathway in a widely distributed intertidal crustacean, the copepod *Tigriopus californicus*. *Proceedings of the National Academy of Sciences of the United States of America. National Academy of Sciences*, *116*(26), 12913–12918. https://doi.org/10.1073/pnas.1819874116

Greenstein, B. J., & Pandolfi, J. M. (2008). Escaping the heat: Range shifts of reef coral taxa in coastal Western Australia. *Global Change Biology*, *14*(3), 513–528. https://doi.org/10.1111/j.1365-2486.2007.01506.x

Hammarlund, E. U., Flashman, E., Mohlin, S., & Licausi, F. (2020). Oxygen-sensing mechanisms across eukaryotic kingdoms and their roles in complex multicellularity. *Science*, *370*(6515), eaba3512. https://doi.org/10.1126/science.aba3512

Hoegh-Guldberg, O., Mumby, P. J., Hooten, A. J., Steneck, R. S., Greenfield, P., Gomez, E., Harvell, C. D., Sale, P. F., Edwards, A. J., Caldeira, K., Knowlton, N., Eakin, C. M., Iglesias-Prieto, R., Muthiga, N., Bradbury, R. H., Dubi, A., & Hatziolos, M. E. (2007). Coral reefs under rapid climate change and ocean acidification. *Science*, *318*(5857), 1737–1742. https://doi.org/10.1126/science.1152509

Honjo, K., Arai, Y., Tsuchida, S., Nakagawa, S., Inoue, H., Saito, M., Ichimaru, S., Shimomura, S., Inoue, A., Terauchi, R., Mazda, O., & Kubo, T. (2015). HSP70 induced by HIF-1 ALFA regurates anabolic responses in chondrocytes under hypoxic conditions. *Osteoarthritis and Cartilage*, *23*, 154–155. https://doi.org/10.1016/j.joca.2015.02.908

Hoogenboom, M. O., Frank, G. E., Chase, T. J., Jurriaans, S., Álvarez-Noriega, M., Peterson, K., Critchell, K., Berry, K. L. E., Nicolet, K. J., Ramsby, B., & Paley, A. S. (2017). Environmental drivers of variation in bleaching severity of Acropora species during an extreme thermal anomaly. *Frontiers in Marine Science*, *4*(NOV). https://doi.org/10.3389/fmars.2017.00376

Hughes, D. J., Alderdice, R., Cooney, C., Kühl, M., Pernice, M., Voolstra, C. R., & Suggett, D. J. (2020). Coral reef survival under accelerating ocean deoxygenation. *Nature Climate Change*, *10*(4), 1–12. https://doi.org/10.1038/s41558-020-0737-9

Hughes, T. P., Anderson, K. D., Connolly, S. R., Heron, S. F., Kerry, J. T., Lough, J. M., Baird, A. H., Baum, J. K., Berumen, M. L., Bridge, T. C., Claar, D. C., Eakin, C. M., Gilmour, J. P., Graham, N. A. J., Harrison, H., Hobbs, J.-P., Hoey, A. S., Hoogenboom, M., Lowe, R. J., … Wilson, S. K. (2018). Spatial and temporal patterns of mass bleaching of corals in the Anthropocene. *Science*, *359*(6371), 80–83. https://doi.org/10.1126/science.aan8048

Hughes, T. P., Kerry, J. T., Álvarez-Noriega, M., Álvarez-Romero, J. G., Anderson, K. D., Baird, A. H., Babcock, R. C., Beger, M., Bellwood, D. R., Berkelmans, R., Bridge, T. C., Butler, I. R., Byrne, M., Cantin, N. E., Comeau, S., Connolly, S. R., Cumming, G. S., Dalton, S. J., Diaz-Pulido, G., … Wilson, S. K. (2017). Global warming and recurrent mass bleaching of corals. *Nature*, *543*(7645), 373–377. https://doi.org/10.1038/nature21707

Hume, B. C. C., Smith, E. G., Hugh, M. Z., Warrington, J. M., Burt, J. A., LaJeunesse, T. C., Wiedenmann, J., & Voolstra, C. R. (2019). SymPortal: A novel analytical framework and platform for coral algal symbiont next-generation sequencing *ITS2* profiling. *Molecular Ecology Resources*, *19*(4), 1063–1080. https://doi.org/10.1111/1755-0998.13004

Hur, E., Kim, H.-H., Choi, S. M., Kim, J. H., Yim, S., Kwon, H. J., Choi, Y., Kim, D. K., Lee, M.-O., & Park, H. (2002). Reduction of hypoxia-induced transcription through the repression of hypoxia-inducible factor-1α/aryl hydrocarbon receptor nuclear translocator DNA binding by the 90-kDa heat-shock protein inhibitor radicicol. *Molecular Pharmacology*, *62*(5), 975–982. https://doi.org/10.1124/mol.62.5.975

Iorio, J., Petroni, G., Duranti, C., & Lastraioli, E. (2019). Potassium and sodium channels and the Warburg effect: Biophysical regulation of cancer metabolism. *Bioelectricity*, *1*(3), 188–200. https://doi.org/10.1089/bioe.2019.0017

Isaacs, J. S., Jung, Y.-J., Mimnaugh, E. G., Martínez, A., Cuttitta, F., & Neckers, L. (2002). Hsp90 regulates a von Hippel Lindau-independent hypoxia-inducible factor-1 alpha-degradative pathway. *The Journal of Biological Chemistry*, *277*(33), 29936–29944. https://doi.org/10.1074/jbc.M204733200

Jackson, J. B. C. (2008). Ecological extinction and evolution in the brave new ocean. *Proceedings of the National Academy of Sciences of the United States of America*, *105*(Suppl. 1), 11458–11465. https://doi.org/10.1073/pnas.0802812105

Jeffrey, S. W., & Humphrey, G. F. (1975). New spectrophotometric equations for determining chlorophylls a, b, c1 and c2 in higher plants, algae and natural phytoplankton. *Biochemie Und Physiologie Der Pflanzen*, *167*(2), 191–194. https://doi.org/10.1016/s0015-3796(17)30778-3

Kaelin, W. G., & Ratcliffe, P. J. (2008). Oxygen sensing by metazoans: The central role of the HIF hydroxylase pathway. *Molecular Cell*, *30*(4), 393–402. https://doi.org/10.1016/j.molcel.2008.04.009

Kanehisa, M., & Sato, Y. (2020). KEGG Mapper for inferring cellular functions from protein sequences. *Protein Science*, *29*(1), 28–35. https://doi.org/10.1002/pro.3711

Katschinski, D., Le, L. U., Schindler, S., Thomas, T., Voss, A., & Wenger, R. (2004). Interaction of the PAS B domain with HSP90 accelerates hypoxia-inducible factor-1α stabilization. *Cellular Physiology and Biochemistry*, *14*(4–6), 351–360. https://doi.org/10.1159/000080345

Keeling, R. F., Körtzinger, A., & Gruber, N. (2010). Ocean deoxygenation in a warming world. *Annual Review of Marine Science*, *2*(1), 199–229. https://doi.org/10.1146/annurev.marine.010908.163855

Kenkel, C. D., Meyer, E., & Matz, M. V. (2013). Gene expression under chronic heat stress in populations of the mustard hill coral (*Porites astreoides*) from different thermal environments. *Molecular Ecology*, *22*(16), 4322–4334. https://doi.org/10.1111/mec.12390

Klein, S. G., Pitt, K. A., Nitschke, M. R., Goyen, S., Welsh, D. T., Suggett, D. J., & Carroll, A. R. (2017). Symbiodinium mitigate the combined effects of hypoxia and acidification on a noncalcifying cnidarian. *Global Change Biology*, *23*(9), 3690–3703. https://doi.org/10.1111/gcb.13718

Kühl, M., Cohen, Y., Dalsgaard, T., Jørgensen, B. B., & Revsbech, N. P. (1995). Microenvironment and photosynthesis of zooxanthellae in scleractinian corals studied with microsensors for O_2, pH and light. *Marine Ecology Progress Series*, *117*, 159–172. https://doi.org/10.3354/meps117159

Kühl, M., Holst, G., Larkum, A. W. D., & Ralph, P. J. (2008). Imaging of oxygen dynamics within the endolithic algal community of the massive coral *Porites lobata*. *Journal of Phycology*, *44*(3), 541–550. https://doi.org/10.1111/j.1529-8817.2008.00506.x

LaJeunesse, T. C., Parkinson, J. E., Gabrielson, P. W., Jeong, H. J., Reimer, J. D., Voolstra, C. R., & Santos, S. R. (2018). Systematic revision of Symbiodiniaceae s the antiquity and diversity of coral endosymbionts. *Current Biology*, *28*(16), 2570–2580.e6. https://doi.org/10.1016/j.cub.2018.07.008

Langmead, B., & Salzberg, S. L. (2012). Fast gapped-read alignment with Bowtie 2. *Nature Methods*, *9*(4), 357–359. https://doi.org/10.1038/nmeth.1923

Leggat, W., Seneca, F., Wasmund, K., Ukani, L., Yellowlees, D., & Ainsworth, T. D. (2011). Differential responses of the coral host and their algal symbiont to thermal stress. *PLoS One*, *6*(10), e26687. https://doi.org/10.1371/journal.pone.0026687

Levy, O., Kaniewska, P., Alon, S., Eisenberg, E., Karako-Lampert, S., Bay, L. K., Reef, R., Rodriguez-Lanetty, M., Miller, D. J., & Hoegh-Guldberg, O. (2011). Complex diel cycles of gene expression in coral-algal symbiosis. *Science*, *331*(6014), 175. https://doi.org/10.1126/science.1196419

Li, H., Handsaker, B., Wysoker, A., Fennell, T., Ruan, J., Homer, N., Marth, G., Abecasis, G., & Durbin, R. (2009). The sequence alignment/map format and SAMtools. *Bioinformatics*, *25*(16), 2078–2079. https://doi.org/10.1093/bioinformatics/btp352

Liew, Y. J., Zoccola, D., Li, Y., Tambutté, E., Venn, A. A., Michell, C. T., Cui, G., Deutekom, E. S., Kaandorp, J. A., Voolstra, C. R., Forêt, S., Allemand, D., Tambutté, S., & Aranda, M. (2018). Epigenome-associated phenotypic acclimatization to ocean acidification in a reef-building coral. *Science Advances*, *4*(6), eaar8028. https://doi.org/10.1101/188227

Loenarz, C., Coleman, M. L., Boleininger, A., Schierwater, B., Holland, P. W. H., Ratcliffe, P. J., & Schofielda, C. J. (2011). The hypoxia-inducible transcription factor pathway regulates oxygen sensing in the simplest animal, *Trichoplax adhaerens*. *EMBO Reports*, *12*(1), 63–70. https://doi.org/10.1038/embor.2010.170

López-Barneo, J., Pardal, R., & Ortega-Sáenz, P. (2001). Cellular mechanism of oxygen sensing. *Annual Review of Physiology*, *63*(1), 259–287. https://doi.org/10.1146/annurev.physiol.63.1.259

Love, M. I., Huber, W., & Anders, S. (2014). Moderated estimation of fold change and dispersion for RNA-seq data with DESeq2. *Genome Biology*, *15*(12), 550. https://doi.org/10.1186/s13059-014-0550-8

Luo, W., Zhong, J., Chang, R., Hu, H., Pandey, A., & Semenza, G. L. (2010). Hsp70 and CHIP selectively mediate ubiquitination and degradation of hypoxia-inducible factor (HIF)-1α but not HIF-2α. *Journal of Biological Chemistry*, *285*(6), 3651–3663. https://doi.org/10.1074/jbc.M109.068577

Lushchak, V. I., & Bagnyukova, T. V. (2006). Effects of different environmental oxygen levels on free radical processes in fish. *Comparative Biochemistry and Physiology - B Biochemistry and Molecular Biology*, *144*(3), 283–289. https://doi.org/10.1016/j.cbpb.2006.02.014

Matthews, J. L., Oakley, C. A., Lutz, A., Hillyer, K. E., Roessner, U., Grossman, A. R., Weis, V. M., & Davy, S. K. (2018). Partner switching and metabolic flux in a model cnidarian–dinoflagellate symbiosis. *Proceedings of the Royal Society B: Biological Sciences*, *285*(1892), 2336. https://doi.org/10.1098/rspb.2018.2336

Mills, D. B., Francis, W. R., Vargas, S., Larsen, M., Elemans, C. P. H., Canfield, D. E., & Wörheide, G. (2018). The last common ancestor of animals lacked the HIF pathway and respired in low-oxygen environments. *eLife*, *7*, 1–17. https://doi.org/10.7554/elife.31176

Peng, Y., Cui, C., He, Y., Ouzhuluobu, H. Z., Deying Yang, Q. U., Zhang, B., Yang, L., He, Y., Xiang, K., Zhang, X., Bhandari, S., Shi, P., Yangla, D., Baimakangzhuo, D., Pan, Y., Cirenyangji, B., Gonggalanzi, C. B., Bianba, B., Ciwangsangbu, S. X., … Bing, S. U. (2017). Down-regulation of EPAS1 transcription and genetic adaptation of Tibetans to high-altitude hypoxia. *Molecular Biology and Evolution*, *34*(4), 818–830. https://doi.org/10.1093/molbev/msw280

Pernice, M., Dunn, S. R., Miard, T., Dufour, S., Dove, S., & Hoegh-Guldberg, O. (2011). Regulation of apoptotic mediators reveals dynamic responses to thermal stress in the reef building coral *Acropora millepora*. *PLoS One*, *6*(1), e16095. https://doi.org/10.1371/journal.pone.0016095

Pernice, M., Raina, J.-B., Rädecker, N., Cárdenas, A., Pogoreutz, C., & Voolstra, C. R. (2020). Down to the bone: The role of overlooked endolithic microbiomes in reef coral health. *The ISME Journal*, 325–334. https://doi.org/10.1038/s41396-019-0548-z

Poli, D., Fabbri, E., Goffredo, S., Airi, V., & Franzellitti, S. (2017). Physiological plasticity related to zonation affects hsp70 expression in the reef-building coral *Pocillopora verrucosa*. *PLoS One*, *12*(2), e0171456. https://doi.org/10.1371/journal.pone.0171456

Ricci, F., Rossetto Marcelino, V., Blackall, L. L., Kühl, M., Medina, M., & Verbruggen, H. (2019). Beneath the surface: Community assembly and functions of the coral skeleton microbiome. *Microbiome*, *7*(1), 1–10. https://doi.org/10.1186/s40168-019-0762-y

Roberts, A., & Pachter, L. (2013). Streaming fragment assignment for real-time analysis of sequencing experiments. *Nature Methods*, *10*(1), 71–73. https://doi.org/10.1038/nmeth.2251

Ruiz-Jones, L. J., & Palumbi, S. R. (2015). Transcriptome-wide changes in coral gene expression at noon and midnight under field conditions. *Biological Bulletin*, *228*(3), 227–241. https://doi.org/10.1086/BBLv228n3p227

Rytkönen, K. T., Williams, T. A., Renshaw, G. M., Primmer, C. R., & Nikinmaa, M. (2011). Molecular evolution of the metazoan PHD-HIF oxygen-sensing system. *Molecular Biology and Evolution*, *28*(6), 1913–1926. https://doi.org/10.1093/molbev/msr012

Scarpulla, R. C., Vega, R. B., & Kelly, D. P. (2012). Transcriptional integration of mitochondrial biogenesis. *Trends in Endocrinology & Metabolism*, *23*(9), 459–466. https://doi.org/10.1016/j.tem.2012.06.006

Schmidt, R. R., Weits, D. A., Feulner, C. F. J., & van Dongen, J. T. (2018). Oxygen sensing and integrative stress signaling in plants. *Plant Physiology*, *176*(2), 1131–1142. https://doi.org/10.1104/pp.17.01394

Schmidtko, S., Stramma, L., & Visbeck, M. (2017). Decline in global oceanic oxygen content during the past five decades. *Nature*, *542*(7641), 335–339. https://doi.org/10.1038/nature21399

Seneca, F. O., & Palumbi, S. R. (2015). The role of transcriptome resilience in resistance of corals to bleaching. *Molecular Ecology*, *24*(7), 1467–1484. https://doi.org/10.1111/mec.13125

Seveso, D., Montano, S., Maggioni, D., Pedretti, F., Orlandi, I., Galli, P., & Vai, M. (2018). Diel modulation of Hsp70 and Hsp60 in corals living in a shallow reef. *Coral Reefs*, *37*(3), 801–806. https://doi.org/10.1007/s00338-018-1703-0

Shin, D. H.,Lin, H., Zheng, H., Kim, K. S., Kim, J. Y., Chun, Y. S., Park, J. W., Nam, J. H., Kim, W. K., Zhang, Y. H., & Kim, S. J. (2014). HIF-1α–mediated upregulation of TASK-2 K^+ channels augments Ca^{2+} signaling in mouse B cells under hypoxia. *The Journal of Immunology*, *193*(10), 4924–4933. https://doi.org/10.4049/jimmunol.1301829

Suggett, D. J., & Smith, D. J. (2020). Coral bleaching patterns are the outcome of complex biological and environmental networking. *Global Change Biology*, *26*(1), 68–79. https://doi.org/10.1111/gcb.14871

Thomas, L. W., & Ashcroft, M. (2019). Exploring the molecular interface between hypoxia-inducible factor signalling and mitochondria. *Cellular and Molecular Life Sciences*, *76*(9), 1759–1777. https://doi.org/10.1007/s00018-019-03039-y

Tolleter, D., Seneca, F. O., DeNofrio, J. C., Krediet, C. J., Palumbi, S. R., Pringle, J. R., & Grossman, A. R. (2013). Report coral bleaching independent of photosynthetic activity. *Current Biology*, *23*, 1782–1786. https://doi.org/10.1016/j.cub.2013.07.041

Veal, C. J., Carmi, M., Fine, M., & Hoegh-Guldberg, O. (2010). Increasing the accuracy of surface area estimation using single wax dipping of coral fragments. *Coral Reefs*, *29*(4), 893–897. https://doi.org/10.1007/s00338-010-0647-9

Wang, F., Chen, Z.-H., & Shabala, S. (2017). Hypoxia sensing in plants: On a quest for ion channels as putative oxygen sensors. *Plant and Cell Physiology*, *58*(7), 1126–1142. https://doi.org/10.1093/pcp/pcx079

Weis, V. M. (2008). Cellular mechanisms of Cnidarian bleaching: Stress causes the collapse of symbiosis. *Journal of Experimental Biology*, *211*(19), 3059–3066. https://doi.org/10.1242/jeb.009597

Xiang, T., Lehnert, E., Jinkerson, R. E., Clowez, S., Kim, R. G., DeNofrio, J. C., Pringle, J. R., & Grossman, A. R. (2020). Symbiont population control by host-symbiont metabolic interaction in Symbiodiniaceae-cnidarian associations. *Nature Communications*, *11*(1), 1–9. https://doi.org/10.1038/s41467-019-13963-z

Yang, C.-C., Lin, L.-C., Wu, M.-S., Chien, C.-T., & Lai, M.-K. (2009). Repetitive hypoxic preconditioning attenuates renal ischemia/reperfusion induced oxidative injury via upregulating HIF-1α–dependent bcl-2 signaling. *Transplantation*, *88*(11), 1251–1260. https://doi.org/10.1097/TP.0b013e3181bb4a07

Yum, L. K., Baumgarten, S., Röthig, T., Roder, C., Roik, A., Michell, C., & Voolstra, C. R. (2017). Transcriptomes and expression profiling of deep-sea corals from the Red Sea provide insight into the biology of azooxanthellate corals. *Scientific Reports*, *7*(1). https://doi.org/10.1038/s41598-017-05572-x

Zhang, J., & Ney, P. A. (2009). Role of BNIP3 and NIX in cell death, autophagy, and mitophagy. *Cell Death & Differentiation*, *16*(7), 939–946. https://doi.org/10.1038/cdd.2009.16

Ziegler, M., Seneca, F. O., Yum, L. K., Palumbi, S. R., & Voolstra, C. R. (2017). Bacterial community dynamics are linked to patterns of coral heat tolerance. *Nature Communications*, *8*, 14213. https://doi.org/10.1038/ncomms14213

Zoccola, D., Morain, J., Pagès, G., Caminiti-Segonds, N., Giuliano, S., Tambutté, S., & Allemand, D. (2017). Structural and functional analysis of coral Hypoxia Inducible Factor. *PLoS One*, *12*(11), 1–13. https://doi.org/10.1371/journal.pone.0186262

SUPPORTING INFORMATION

Additional supporting information may be found online in the Supporting Information section.

How to cite this article: Alderdice R, Suggett DJ, Cárdenas A, et al. Divergent expression of hypoxia response systems under deoxygenation in reef-forming corals aligns with bleaching susceptibility. *Glob Change Biol*. 2021;27:312–326. https://doi.org/10.1111/gcb.15436